IEEE Access
Multidisciplinary ⋮ Rapid Review ⋮ Open Access Journal

Received June 16, 2019, accepted June 24, 2019, date of publication July 5, 2019, date of current version July 23, 2019.

Digital Object Identifier 10.1109/ACCESS.2019.2926841

Wearable Bioimpedance Measurement for Respiratory Monitoring During Inspiratory Loading

DOLORES BLANCO-ALMAZÁN[1,2,3], WILLEMIJN GROENENDAAL[4], FRANCKY CATTHOOR[5,6], (Fellow, IEEE), AND RAIMON JANÉ[1,2,3], (Senior Member, IEEE)

[1]Institute for Bioengineering of Catalonia, The Barcelona Institute of Science and Technology, 08028 Barcelona, Spain
[2]Department of Automatic Control (ESAII), Universitat Politècnica de Catalunya · Barcelona Tech, 08028 Barcelona, Spain
[3]Biomedical Research Networking Center in Bioengineering, Biomaterials and Nanomedicine, 08028 Barcelona, Spain
[4]Holst Center/IMEC, 5656AE Eindhoven, The Netherlands
[5]IMEC, B-3001 Leuven, Belgium
[6]ESAT-MICAS Laboratory, Katholieke Universiteit Leuven, B-3001 Leuven, Belgium

Corresponding author: Dolores Blanco-Almazán (dblanco@ibecbarcelona.eu)

This work was supported in part by the Universities and Research Secretariat from the Ministry of Business and Knowledge/Generalitat de Catalunya under Grant FI-DGR and Grant GRC 2017 SGR 01770, in part by the Spanish Ministry of Economy and Competitiveness through the MINECO/FEDER Project under Grant DPI2015-68820-R, in part by the Agencia Estatal de Investigación from the Spanish Ministry of Science, Innovation and Universities and the European Regional Development Fund, under Grant RTI2018-098472-B-I00, and in part by the CERCA Programme/Generalitat de Catalunya.

ABSTRACT Bioimpedance is an unobtrusive noninvasive technique to measure respiration and has a linear relation with volume during normal breathing. The objective of this paper was to assess this linear relation during inspiratory loading protocol and determine the best electrode configuration for bioimpedance measurement. The inspiratory load is a way to estimate inspiratory muscle function and has been widely used in studies of respiratory mechanics. Therefore, this protocol permitted us to evaluate bioimpedance performance under breathing pattern changes. We measured four electrode configurations of bioimpedance and airflow simultaneously in ten healthy subjects using a wearable device and a standard wired laboratory acquisition system, respectively. The subjects were asked to perform an incremental inspiratory threshold loading protocol during the measurements. The load values were selected to increase progressively until the 60% of the subject's maximal inspiratory pressure. The linear relation of the signals was assessed by Pearson correlation (r) and the waveform agreement by the mean absolute percentage error (MAPE), both computed cycle by cycle. The results showed a median greater than 0.965 in r coefficients and lower than 11 % in the MAPE values for the entire population in all loads and configurations. Thus, a strong linear relation was found during all loaded breathing and configurations. However, one out of the four electrode configurations showed robust results in terms of agreement with volume during the highest load. In conclusion, bioimpedance measurement using a wearable device is a noninvasive and a comfortable alternative to classical methods for monitoring respiratory diseases in normal and restrictive breathing.

INDEX TERMS Bioimpedance, chronic respiratory diseases, electrode configurations, inspiratory threshold protocol, wearable.

I. INTRODUCTION

Chronic Respiratory Diseases (CRD) are one of the leading causes of morbidity and mortality worldwide. In particular, Chronic Obstructive Pulmonary Disease (COPD) is ranked the 3th cause of deaths worldwide [1]. These diseases are diagnosed and monitored by devices that measure the pulmonary function. These methods are usually uncomfortable and modify the normal breathing of the patients [2]. For instance, spirometry is widely used for COPD or asthma diagnosis and assessment [3]. Despite that, there are more comfortable noninvasive methods capable to extract respiratory-related information like thoracic bioimpedance, inductance plethysmography or electromyography, but they are not as widespread as classical ones because of the lack of evidence in clinical applications [4]. Consequently, there is

The associate editor coordinating the review of this manuscript and approving it for publication was Ming Luo.

a need to validate unobtrusive methods to be used in CRD diagnosis and monitoring. In the presented study, thoracic bioimpedance was selected because of its suitability for continuous respiratory monitoring.

Bioimpedance is a noninvasive and comfortable technique for measuring impedance changes. Previous studies reported its linear relation with respiratory volume [5]–[11] and its capability to obtain typical respiratory parameters [12]–[15] when bioimpedance was measured in the thorax. Accordingly, bioimpedance has a strong linear relation with respiratory volume. Not all of these studies included the validation of bioimpedance in different respiratory conditions, Cohen *et al.* included complete simulated airway obstruction [6] and Marmberg *et al.* focused on infants with recurrent airway symptoms [15]. Inspiratory threshold loading protocols enable the study of ventilatory responses imposing inspiratory loads to the subjects. This kind of protocol is associated with changes in breathing pattern [16] and diaphragm fatigue [17]. Therefore, the use of inspiratory loading permitted to understand better the effects of this respiratory loads in breathing mechanics in the same way as an airway obstruction could do. Other respiratory studies [16]–[22] analyzed breathing pattern changes when subjects breathed following this kind of protocol but none measured bioimpedance.

Another important issue in bioimpedance measurement is its sensitivity to electrode location. Thoracic bioimpedance measurement is a combination of the impedance of different body tissues, such as the lungs, the heart muscle or the liver and also blood and air. These contributions were studied in different electrode locations by computer simulations in an human thorax model [23]–[25]. The simulations showed that middle thoracic electrode locations can provide values reflecting relative impedance changes of the lungs [23]. Previous studies including human subjects compared bioimpedance performance regarding to respiration in different electrode locations [8]–[10], [14]. Seppä *et al.* compared the lateral configurations to anteroposterior ones and lateral configurations showed better performance [9] and specifically the one which combines thorax and arms [10]. De Cannière *et al.* tested different configurations and the performance and subject comfort were better when the electrodes were in the midaxillary line at intercostal line [14]. Moreover, bioimpedance can be easily measured using a wearable device [14], [26], [27] which is an advantage over classical methods for monitoring respiratory function.

The novelty of the presented study is the investigation of bioimpedance for respiratory monitoring during restrictive breathing conditions. The main objectives of this study are to assess the linear relation between bioimpedance and volume during a inspiratory loading protocol and determine the best electrode configuration in these respiratory conditions. So our main contribution is to propose simpler methods to accurately monitor the respiratory conditions of CRD patients. In addition, we evaluated the viability of this approach with practical experiments. Good results in this study support the use of bioimpedance in ambulatory measurements using wearable devices.

II. MATERIALS AND METHODS

A. SUBJECTS

Ten healthy subjects (4 females and 6 males) volunteered to participate in the study. The age range of the subjects was [24 – 37] (mean ± standard deviation: 30.5± 5.1) and the body mass index range was [19.5 – 26.8] (mean ± standard deviation: 23.1 ± 2.59). None were smoker or reported any respiratory disease.

The study was approved by the Institutional Review Board of the Institute for Bioengineering of Catalonia. The measurement and protocol procedure were described in an accessible document by the subjects and written consent was obtained from each subject.

B. RESPIRATORY PROTOCOL

The subjects were asked to perform an inspiratory threshold loading protocol during the measurements. This protocol was used in [22] but it did not include bioimpedance measurement.

Before starting the protocol, the subjects performed a maximal respiratory maneuver to get their maximal static inspiratory pressure (MIP) from functional residual capacity [28]. The protocol consisted of imposing five inspiratory threshold loads to the subjects while breathing. The five loads values corresponded to a percentage of each subject's MIP. The loads were chosen to increase progressively, and the threshold values were 12 % (L1), 24 % (L2), 36 % (L3), 48 % (L4) and 60 % (L5) of subject's MIP. The protocol started recording subject's quiet tidal breathing (QB) for 2 minutes and after that the inspiratory threshold loads were imposed. The subjects breathed 30 times per load and each load was followed by a resting time for the subjects to return to baseline.

During the measurements, the subjects were comfortably seated in an upright position and wore a nose clip to avoid nasal breathing.

C. EQUIPMENT

A wearable device and a standard wired laboratory acquisition system were used to record physiological data. The combination of the two systems permitted us to compare the wearable device performance to a reference one and to validate its use for hospital environments.

The wearable device (Stichting imec The Netherlands) was used to measure bioimpedance. The device includes the MUSEIC v1 chip [27] and is capable of recording more than one configuration simultaneously switching the current injection and voltage measurement between the different configurations. This allows isolated bioimpedance values from each configuration over the time. The excitation current amplitude was 110 μA at 80 kHz frequency. Stress test AG/AgCl electrodes (EL501, Biopac Systems, Inc. Goleta, CA, USA) were used for bioimpedance measurement.

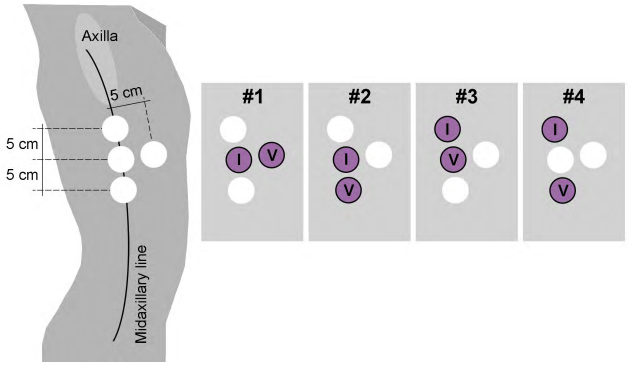

FIGURE 1. Representation of the four tetra-polar electrode configurations. Only the right side is shown because the configurations were symmetric from the midsternal line. #1, #2, #3, and #4 denote the electrode configurations where the used electrodes are highlighted, *I* refers to the injecting electrodes and *V* to the voltage measurement electrodes.

Airflow was measured with Biopac transducer (pneumotach transducer TSD107B, Biopac Systems, Inc.). The airflow signal was amplified 1000 times, filtered by a 300 Hz low-pass analog filter (DA100C, Biopac Systems, Inc.) and A/D converted with a Biopac MP150 system. The subjects breathed through a mouth piece which included a bacterial filter.

Electrocardiogram (ECG) signals were recorded using the wearable device (Stichting imec, The Netherlands) and the standard wired system (ECG100C, Biopac Systems, Inc.).

An inspiratory muscle trainer (POWERbreathe KH2, POWERbreathe International Ltd, Southam, UK) was used to perform the MIP respiratory maneuver and to impose inspiratory threshold loads during the protocol. This trainer is a class 1 medical device which is electronically controlled to impose the threshold resistance.

D. ELECTRODE CONFIGURATIONS

Four tetrapolar electrode configurations were used to record bioimpedance signal from different thorax zones (Fig. 1) based on previous studies [10], [14]. Tetrapolar configuration uses two leads for injecting the excitation current (I) and the other two to measuring the voltage generated (V). Having different configurations allowed the comparison between their performance and their applicability in load respiratory conditions.

All electrode configurations were symmetric from the midsternal line. Configuration 1 was horizontal; the injecting electrodes were placed one on each midaxillary line at approximately 7 cm from the end of axilla. The voltage electrodes were horizontally placed at 5 cm from the injecting ones, closer to the midsternal line. Configurations 2, 3 and 4 were vertical, so all electrodes were placed on the midaxillary lines. The injecting current electrodes were the upper ones. In Configurations 2 and 3, the voltage electrodes were separated 5 cm from the injecting ones, but Configuration 3 zone was closer to the axilla (Fig. 1). The electrodes of configuration 4 were separated 10 cm on the midaxillary line, so this configuration covered a broader zone. The differences in geometry and distances of the configurations permitted to verify whether that can help to further improve the accuracy and robustness of the monitoring.

E. SIGNAL PROCESSING

The first step was to synchronize signals from both systems using the cross-correlation of the ECG signals. The lag which maximizes the cross-correlation corresponded to the delay between the signals from the systems.

Bioimpedance signals were sampled at 16 Hz. After digitalization, the bioimpedance channels were high-pass filtered (zero-phase 8th order Butterworth, $fc = 0.1$ Hz) to reduce baseline oscillations. The 8th order was chosen to have a narrow bandwidth. A lower order could be used as well for the purpose of this study. A cut-off frequency of 0.1 Hz was selected. A higher value could remove respiratory information from the bioimpedance signal. To increase the time resolution, the bioimpedance signal was interpolated with sampling frequency of 200 Hz by cubic interpolation.

Airflow signal decimated from 10 kHz to 200 Hz after being low-pass filtered to avoid aliasing. The airflow information is in the low frequencies; therefore, the airflow signal was low-pass filtered (zero-phase 8th order Butterworth, $fc = 5$ Hz) to remove the high-frequency content. The volume signal was calculated by the trapezoidal numerical integration of the low-pass filtered flow signal.

Thereafter, volume and bioimpedance signals were low-pass filtered (zero-phase 8th order Butterworth, $fc = 5$ Hz) and high-pass filtered (zero-phase 8th order Butterworth, $fc = 0.1$ Hz). Additionally, bioimpedance was smoothed applying a moving average of 1 s. Both signals were normalized dividing them by their root mean-squared value.

The signals were segmented into respiratory cycles using airflow as the reference signal. On several occasions the bioimpedance signal showed to be delayed or advanced in relation to volume signal, especially when a high load was imposed to some subjects. To better compare the respiratory cycles of volume and bioimpedance signals, we calculated these time differences using the cross-correlation of bioimpedance and volume for each cycle individually. Then, each delay (δ_i, i is the cycle number) was the lag which maximizes the cross-correlation. To have coherent delays over respiratory cycles, we also computed the global delay for each load (Δ_L, L is the load number) and used it to limit the range of δ_i. We tested several ranges and we got precise results when the δ_i were in the range $[\Delta_L \pm N/4]$, where N is the length of the cycle in samples. The cycle onsets of bioimpedance signal were modified according to the obtained delays, getting the signals aligned in each respiratory cycle.

The signal processing was performed using MATLAB (v. R2018a, Natick, MA, USA) for each load separately.

F. STATISTICAL ANALYSIS

The linear relationship between volume and bioimpedance signals was evaluated computing Pearson correlation. Pearson correlation coefficient (r) takes values on the

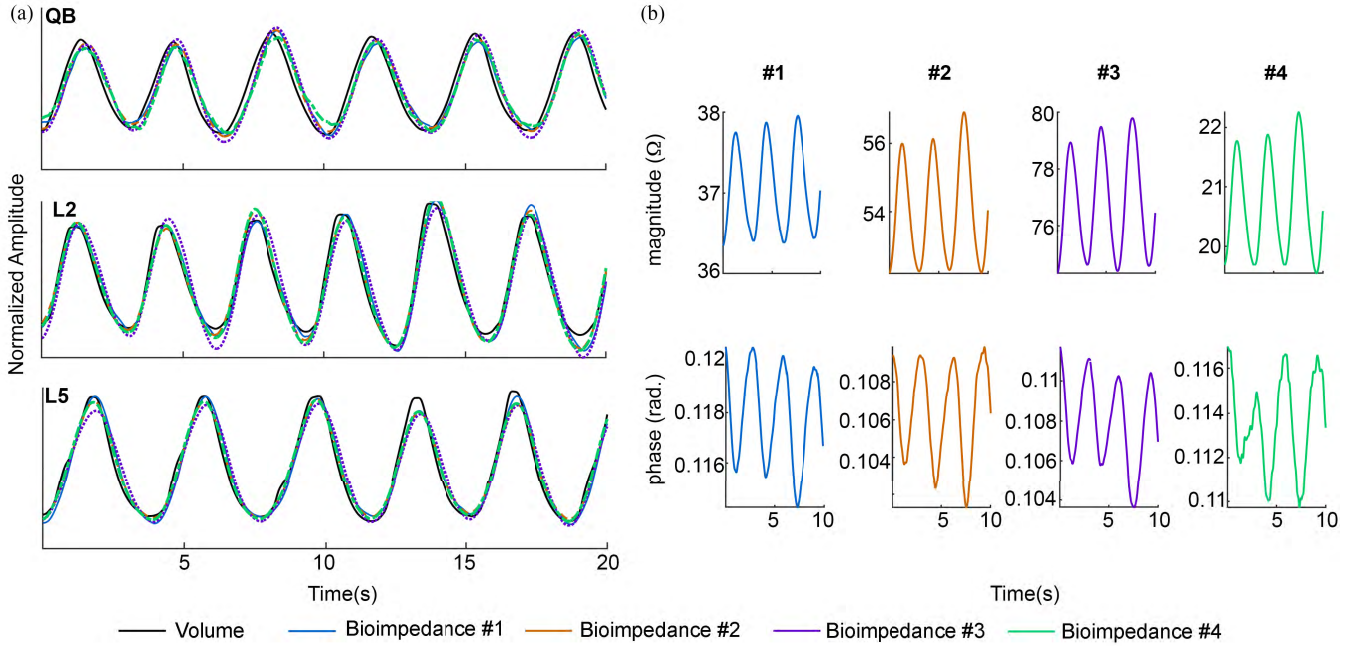

FIGURE 2. Temporal representation of volume and bioimpedance signals of subject S04 after signal processing. (a) The signals correspond to QB, L2, and L5 threshold values of the respiratory protocol. (b) Magnitude and phase of bioimpedance for the four configurations. The signals correspond to the L2 and only for this representation were not high-pass filtered to maintain the impedance values.

range [-1, 1], meaning 0 the signals were uncorrelated, -1 negatively correlated and 1 positively correlated. The Pearson correlation coefficient was calculated for each segmented respiratory cycle after delay correction as follows,

$$r_i = \frac{\sum_{n=1}^{N}(V_i[n] - \overline{V}_i)(Z_i[n] - \overline{Z}_i)}{\sqrt{\sum_{n=1}^{N}(V_i[n] - \overline{V}_i)^2 \sum_{n=1}^{N}(Z_i[n] - \overline{Z}_i)^2}} \quad (1)$$

where V_i and Z_i are the volume and bioimpedance signals during cycle number i, N the number of samples, and $\overline{V}_i$ and $\overline{Z}_i$ their mean value in cycle i.

The coefficient of determination, r^2, and simple linear regression were also used to assess the linearity when the volume and bioimpedance values are represented together in the same chart.

Mean Absolute Percentage Errors (MAPE) were computed between volume and bioimpedance for each respiratory cycle. The error percentage was related to the maximum value of the volume in each cycle.

$$MAPE_i(\%) = 100\frac{1}{N}\sum_{n=1}^{N}\left|\frac{V_i[n] - Z_i[n]}{max(V_i[n])}\right| \quad (2)$$

Median, first and third quartile (Q1, Q3) of the cycle correlation coefficient and MAPE data were computed to quantify the tendency and distribution of these measures.

III. RESULTS

Four different electrode configurations of bioimpedance and airflow were measured simultaneously in 10 healthy subjects during incremental inspiratory threshold loading protocol. Bioimpedance linearity was assessed with volume signal which was obtained from airflow by trapezoidal numerical integration.

Volume and bioimpedance signals are represented in Fig. 2a for subject S04 during QB, L2 and L5. This subject was representative of most subjects in which the waveforms of volume and bioimpedance showed a good similarity in all configurations and loads. Fig.2b shows the impedance magnitude and phase for the same subject during L2.

The Pearson correlation coefficients were computed to evaluate the linear relationship between volume and bioimpedance. The correlation coefficients of the signals are represented in Fig. 3 for entire respiratory cycles and for inspiratory and expiratory phases. The correlation between bioimpedance and volume was high being the median greater than 0.965 for the entire population in all loads and configurations (Fig. 3). The r values for entire respiratory cycles showed the same behavior for the four electrode configurations: the r values increased from QB to L1, they were very similar in L1, L2 and L3 and then the values showed a decreasing tendency from L4 to L5. This behavior was also exhibited in correlations computed using only inspirations, but not in expirations which differs in some loads. In every case, the r values showed the decreasing tendency from L3. Note that the r values computed only in inspiratory and expiratory phases were higher than the ones computed using the entire respiratory cycle (Fig. 3).

Correlation results for each single subject from the four configurations are represented in Table 1. According to these

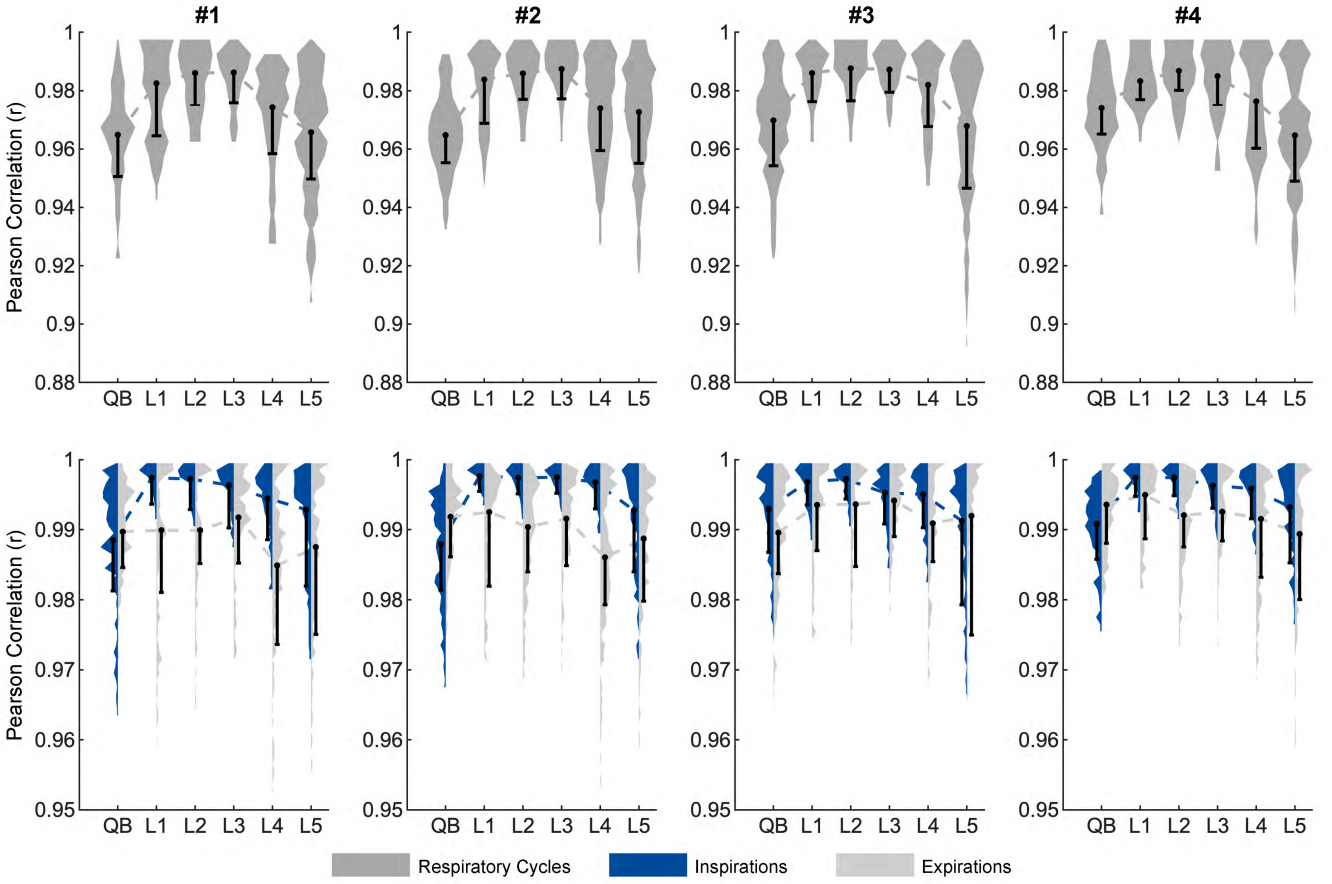

FIGURE 3. Distribution of the Pearson correlation coefficients during inspiratory threshold loading protocol in four electrode configurations. #1, #2, #3, and #4 denote the electrode configurations and QB, L1, L2, L3, L4, and L5 the imposed threshold inspiratory loads. The upper charts include the correlations coefficients computed for the entire respiratory cycles and the lower ones for inspirations and expirations. The distribution of the values are widthwise represented by a normalized histogram, meaning the wider values are more frequent. The median, first quartile and line of tendency are superimposed to the distribution values.

TABLE 1. Pearson correlation *r* of volume and bioimpedance respiratory cycles.

S	Electrode Configurations			
	#1	#2	#3	#4
01	0.978 (0.961)	0.975 (0.966)	0.983 (0.979)	0.981 (0.973)
02	0.949 (0.921)	0.928 (0.870)	0.977 (0.961)	0.974 (0.961)
03	0.975 (0.964)	0.978 (0.967)	0.980 (0.969)	0.982 (0.972)
04	0.971 (0.966)	0.988 (0.978)	0.961 (0.954)	0.990 (0.976)
05	0.983 (0.973)	0.972 (0.961)	0.978 (0.961)	0.979 (0.960)
06	0.981 (0.965)	0.983 (0.970)	0.977 (0.958)	0.985 (0.971)
07	0.986 (0.982)	0.994 (0.990)	0.993 (0.990)	0.997 (0.995)
08	0.949 (0.932)	0.955 (0.937)	0.947 (0.920)	0.960 (0.940)
09	0.991 (0.988)	0.982 (0.973)	0.993 (0.990)	0.972 (0.964)
10	0.984 (0.967)	0.979 (0.964)	0.989 (0.979)	0.977 (0.966)

"S" indicates the subject number. #1, #2, #3 and #4 denote the electrode configurations shown in Fig. 1. The Pearson correlations r are expressed as median and first quartile.

results, the maximum inter-subject coefficient of variation (standard deviation over mean) was highest for configuration 2 (1.95%) and lowest for configuration 4 (1.01%).

The relation between volume and bioimpedance signals is shown in Fig. 4. Simple linear regression was compute for each load and configuration including all the subjects cycles to find the straight line that best fits the data. The strength of the relationship was quantified by the coefficient of determination. The resultant coefficients of determination, r^2, (median and interquartile range) were 0.88 (0.84 to 0.91). L1, L2 and L3 showed high r^2 values where L1 showed the highest. On the contrary, L5 showed the lowest ones. On the other hand, none of the electrode configurations was clearly superior to the others, and all showed similar behavior.

Temporal representation of normalized volume and bioimpedance of subjects S07 and S08 is shown in Fig. 5 during the highest load (L5). S07 is an example of the predominant behavior in the data, showing good agreement between volume and bioimpedance. In contrast, S08 was one of the two subjects that showed a change in bioimpedance waveform for the measurements with configurations 2, 3 and 4 but not for the measurements with configurations 1. This behavior was quantified by MAPE values in Fig. 6 for subjects S07 and S08. Table 2 shows the MAPE values for all subjects and for configuration 1. The range of each subject

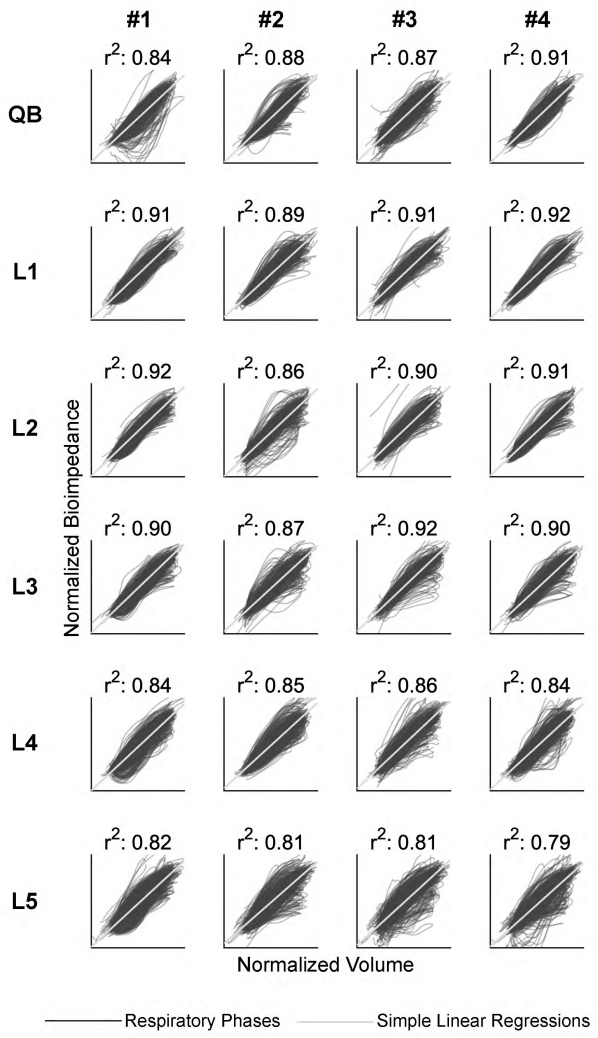

FIGURE 4. Volume and bioimpedance relation during inspiratory threshold loading protocol in four electrode configurations. #1, #2, #3, and #4 denote the electrode configurations and QB, L1, L2, L3, L4, and L5 the imposed threshold inspiratory loads. Each chart includes normalized volume and normalized bioimpedance from respiratory cycles of all subjects, their corresponding simple linear regression and coefficient of determination r^2. Only cycles which correlation are higher to 0.5 are represented.

MAPE values for this configuration were approximately the same through all inspiratory loads.

IV. DISCUSSION

The goal of this study was to assess the linear relationship between bioimpedance and volume during inspiratory loading protocol and conclude the best electrode configuration under these respiratory conditions. We tested the suitability of bioimpedance measurement during incremental inspiratory threshold loading protocol in four electrode configurations (Fig. 1). Incremental inspiratory loading protocols produce breathing pattern changes [16] and diaphragm fatigue [17] and these effects in bioimpedance measurement and in its relation with volume were not analyzed before the presented study.

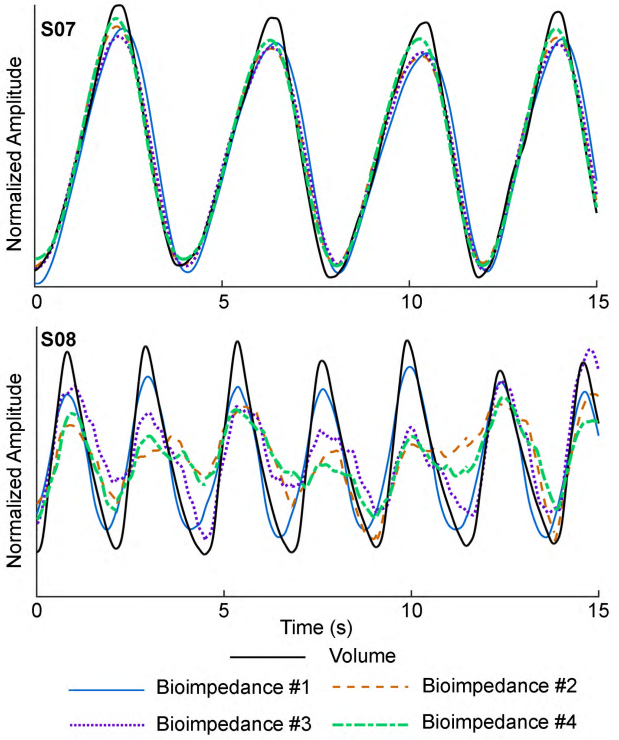

FIGURE 5. Temporal representation of volume and bioimpedance signals of subjects S07 and S08. The signals correspond to the highest load (L5).

The agreement between signals was excellent, the median of the correlation coefficients was greater than 0.965 in all cases for the entire population (Fig. 3). The presented results are comparable to the ones reported by similar studies. In particular, Grenvik *et al.* [5], Ernst *et al.* [7], Seppä *et al.* [8], [10] and Liu *et al.* [11] reported values of correlations between volume and bioimpedance signals as well. We observed differences in the performance of configurations 2 and 3 in comparison to [10] which will be discussed further. Houtven *et al.* [12] and Koivumaki *et al.* [13] extracted features from bioimpedance like respiratory rate and peak-to-peak amplitude and their results were comparable with the ones computed with volume. However, all these studies were developed in free and variable volume breathing but without any loads.

In the field of noninvasive respiratory monitoring, recent studies presented noncontact methods to extract breathing-related information based on depth camera, optical imaging or Doppler radar technologies [29]–[31]. These studies showed promising results but they are limited to the fixed location where the sensors are, and moderate movement conditions. Consequently, the use of noncontact methods are suitable for applications like sleep monitoring or automotive environment. On the other hand, wearable technology allows its use in any location since the user wears the sensors.

The classical methods to monitor and diagnose CRD diseases imply the use of obtrusive techniques. Commonly this techniques are uncomfortable and change the patient's breathing [2]. Therefore, the use of noninvasive techniques like wearable bioimpedance will improve the respiratory

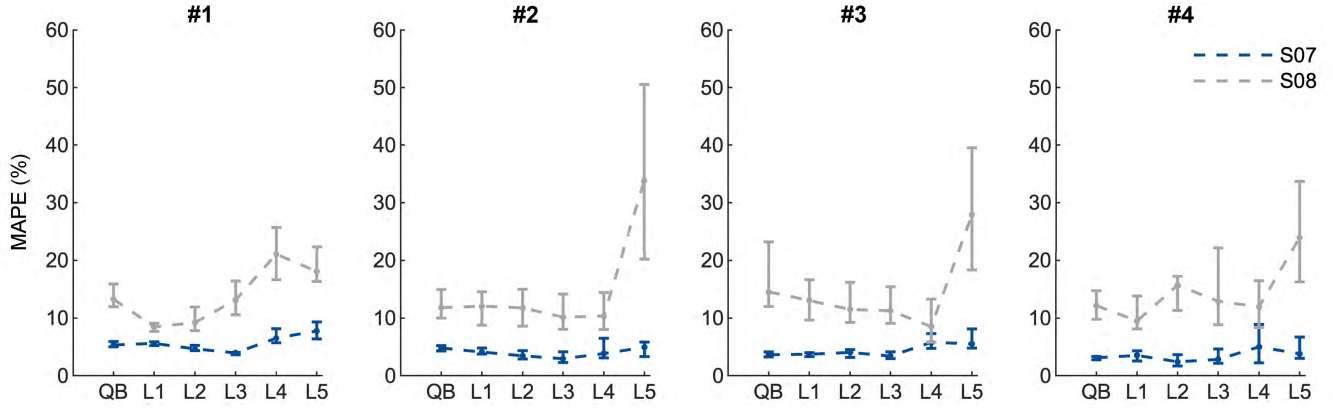

FIGURE 6. Mean Absolute Percentage Errors during inspiratory threshold loading protocol in four electrode configurations for subjects S07 and S08. #1, #2, #3 and #4 denote the electrode configurations and QB, L1, L2, L3, L4, and L5 the imposed threshold inspiratory loads. The errors were computed for the entire respiratory cycles and the percentage is related to the maximum normalized volume value in each cycle.

monitoring in terms of patient's comfort and ability to measure normal breathing. The reported results support the appropriate use of bioimpedance as measure for respiratory monitoring. Specifically, our study also supports its use in different respiratory conditions like imposed inspiratory loads to the subjects. Hence, bioimpedance measurement can be a simpler method to accurately monitor different respiratory conditions in CRD patients.

A. INSPIRATORY LOADING PROTOCOL

The incremental inspiratory threshold loads are associated with changes in the breathing of the subjects who adapt their respiratory pattern to overcome each imposed load and optimize muscle force [16]. Despite the inspiratory loads, bioimpedance signal performed excellently in intermediate inspiratory loads (L1, L2 and L3) getting a median of correlation coefficient greater than 0.983 in all configurations for the entire population (Fig. 3). During the highest loads (L4 and L5) the median for the entire population was greater than 0.965. Hence, the bioimpedance performed well but the correlation values were a bit lower. Especially in L5 load, two subjects (S02 and S08) presented a notable error increase (Fig. 6) due to changes in bioimpedance signal morphology as shown in Fig. 5.

The correlation between volume and bioimpedance signals in quiet breathing was lower than intermediate loads in most subjects (Fig. 3). During QB subjects normally inhaled less volume than when loads were imposed to them and the volume-related bioimpedance changes were consequently lower. Therefore, the reduction in performance of the bioimpedance during QB can be explained because of the low signal-to-noise ratio. Seppä *et al.* noticed this by an improving of the agreement between airflow and airflow-related bioimpedance signal was better at higher tidal volumes [9].

Our results are sufficiently convincing to consider the viability of bioimpedance for respiration monitoring. However, further studies including adult patients with airway obstruction or CRD are needed to validate the suitability of bioimpedance to monitor respiration in adult population. In [15] Malmberg *et al.* showed that bioimpedance derived flow profiles were consistent in most infants although could be less reliable in infants with evident airway obstruction. The differences between [15] and the presented study are notable. For instance, the age of the subjects is relevant because the maturity of pulmonary system is different for infants from 5 to 28 months than for adults. Moreover, the diseases included in [15] might affect differently than CRD in adult population.

We observed a convincing agreement between the signals for all the subjects even when the highest load was imposed. Therefore, we suggest bioimpedance as simple method for respiratory monitoring in free and loaded breathing.

B. ELECTRODE CONFIGURATIONS

Bioimpedance measurement is very dependent on electrode configurations. The effect of electrode configurations were analyzed in previous studies during respiratory maneuvers which included free and variable volume breathing [8]–[10], [14]. Cohen *et al.* also included complete simulated airway obstruction in their protocol [6]. We studied the repercussion of four electrode configurations based on previous studies [10], [14] to compare the performance when an inspiratory load is imposed. Globally none of the electrode configuration showed a superior performance with respect to linearity (Fig. 4) which correlation values were above 0.965 (Fig. 3). These results differ from [10] in which configuration 2 and 3 exhibited a concave relation between volume and bioimpedance signals. Seppä *et al.* explained the potentially reasons of these nonlinear relations as the effect of the movement of the thorax, the diaphragm, or the liver, and the inhomogeneous ventilation distribution. We did not observe these nonlinearities in configuration 2 and 3 and it could be because of the differences between studies. The main difference is the protocol used during bioimpedance measurement. In [10] the subjects performed a forced maximal maneuver and consequently, their thorax and thoracic organs could move more than in our study in which the subjects were free to adopt any breathing pattern to overcome the

TABLE 2. MAPE(%) from volume and bioimpedance respiratory cycles.

S	Inspiratory Threshold Loads					
	QB	L1	L2	L3	L4	L5
01	7.26 (6.50 - 7.96)	8.58 (7.82 - 10.18)	8.60 (7.55 - 10.58)	6.25 (5.26 - 7.65)	10.75 (10.21 - 11.66)	11.06 (10.71 - 12.03)
02	53.51 (34.53 - 65.33)	14.90 (13.32 - 15.88)	10.90 (9.84 - 11.71)	10.93 (10.42 - 12.03)	19.30 (15.32 - 21.50)	17.68 (16.49 - 21.92)
03	7.77 (7.12 - 8.50)	9.49 (8.49 - 10.59)	6.90 (5.34 - 11.66)	5.26 (4.38 - 9.46)	7.05 (5.81 - 7.95)	11.93 (7.92 - 17.32)
04	8.17 (7.81 - 9.16)	7.94 (6.93 - 8.34)	8.30 (7.42 - 9.05)	7.30 (6.86 - 8.08)	7.44 (6.90 - 7.95)	7.97 (6.75 - 9.08)
05	8.44 (7.56 - 9.20)	3.11 (2.09 - 4.57)	5.55 (4.82 - 6.13)	6.94 (5.61 - 10.30)	9.80 (8.64 - 10.67)	11.68 (9.89 - 16.15)
06	8.07 (7.64 - 9.35)	8.00 (6.44 - 9.96)	4.41 (3.73 - 5.02)	6.44 (4.95 - 10.55)	5.63 (5.13 - 7.45)	8.32 (7.08 - 9.74)
07	5.32 (4.99 - 5.93)	5.60 (5.22 - 5.87)	4.64 (4.34 - 5.25)	3.95 (3.63 - 4.03)	6.52 (5.71 - 8.13)	7.74 (6.38 - 9.31)
08	13.25 (11.96 - 15.91)	8.45 (7.68 - 9.10)	9.21 (7.81 - 11.90)	13.14 (10.55 - 16.41)	21.08 (16.64 - 25.70)	18.08 (16.33 - 22.33)
09	4.68 (4.11 - 5.25)	4.95 (2.49 - 7.48)	2.71 (2.22 - 3.65)	5.18 (4.28 - 6.02)	5.83 (4.77 - 6.73)	3.88 (3.25 - 4.90)
10	7.77 (7.25 - 8.83)	4.63 (4.00 - 5.69)	3.47 (2.68 - 4.78)	7.11 (4.62 - 8.90)	10.39 (7.68 - 13.34)	10.28 (9.38 - 12.92)

"S" indicates the subject number. QB, L1, L2, L3, L4 and L5 denote the imposed threshold inspiratory loads to the subjects. The values are related to the configuration 1 and they are expressed as median (first quartile - third quartile).

loads and forced maximal respiration is not usually necessary. Respiratory disease diagnosis requires this test and might limit the use of bioimpedance in that case. On the contrary, our study did not include forced maximal respiration and we show that bioimpedance linearity with volume is good during normal and loaded breathing.

During incremental inspiratory loading protocol, shortness of breath is induced by increasing the breathing effort and the breathing pattern could change to optimize muscle strength [16]. This behavior could interfere in bioimpedance, specially at high loads. The breathing pattern changes could be the reason why bioimpedance waveform worsened in configurations 2, 3 and 4 for subjects S02 and S08 as Fig. 5 shows for S08. Because of this reduce in signal quality, the MAPE values were higher in subjects S02 and S08 during the highest load in configurations 3 and 4, and for subject S08 also in configuration 2 (Fig. 6). Note that the subjects whom performed worse at highest loads (S02 and S08) also had higher overall MAPE values, as Table 2 summarized. The breathing pattern changes could modify the contributions of the different body tissues in bioimpedance measurement. Computer simulations in human thorax models are a tool to understand the contributions of the different body tissues in bioimpedance measurement [23]–[25]. However, these simulations are not practical to model each personalized breathing pattern of the subjects.

Configuration 2 showed an unusual behavior for one subject, bioimpedance values of subject S02 varied contrary to the expected; bioimpedance decreased during inspiration and increased during expiration. We inverse the bioimpedance values for the subject S02 only in configuration 2 to get the expected relation with volume. On the other hand, the signal quality of bioimpedance for subject S02 in configuration 1 was lower for unknown reasons, but only in quiet breathing. The low signal quality causes the high MAPE values in Table 2 (median 53.51).

The four electrode configurations showed a good correlation between bioimpedance and volume in quiet and loaded breathing. We observed reduction in bioimpedance signal quality only in two of the ten subjects in configurations 2, 3 and 4. Despite that, the median of the correlation coefficients for these subjects was above 0.916 at the highest load. Consequently, configuration 1 showed a robust performance in terms of agreement with volume in all subjects although in some cases did not perform the best. The rest of the configurations could provide additional information and be useful in other applications, like in airway obstruction diseases. Along these lines, further studies including patients are needed.

V. LIMITATIONS OF THE STUDY

The presented study showed the linear relationship between bioimpedance and volume during inspiratory loaded breathing in ten healthy subjects. Patients with CRD such as COPD, can have different anthropometry than the healthy subjects included in this study. However, the anthropometry of our healthy subjects can be similar to the anthropometry of many other types of patients. For example, patients with CRD like asthma, or other pulmonary diseases that can affect to everyone, like pneumonia. Inspiratory loads entailed changes in the subjects' breathing and during these changes the agreement between bioimpedance and volume remained good. Including CRD patients could provide an additional validation because of the differences with healthy subjects, especially in their airway obstructions. We think that the presented results represent a benefit of bioimpedance use in respiratory monitoring and early diagnosis. Additional studies with patients should be performed to reinforce these results.

VI. CONCLUSION

This study demonstrated the suitability of bioimpedance for respiratory monitoring in changes of respiratory pattern when inspiratory loads were imposed. The relationship between bioimpedance and volume was clearly linear during the inspiratory threshold loading, even in the highest load (60 % of MIP). None of the four configurations was clearly superior to the others in terms of accuracy, but configuration 1 showed a

more robust performance in terms of agreement with volume when the highest load was imposed.

Therefore, we conclude bioimpedance measured from the electrode configurations used in the presented study is an appropriate method which can be a noninvasive alternative to monitor respiration during loaded breathing. We suggest wearable bioimpedance measurement as convenient and comfortable ambulatory technique to be used for healthcare monitoring of respiratory diseases in normal and restrictive breathing.

REFERENCES

[1] P. R. Lozano, M. Naghavi, K. Foreman, S. Lim, P. K. Shibuya, P. V. Aboyans, J. Abraham, T. Adair, P. R. Aggarwal, S. Y. Ahn, M. A. AlMazroa, M. Alvarado, P. H. R. Anderson, L. M. Anderson, K. G. Andrews, C. Atkinson, P. L. M. Baddour, S. Barker-Collo, and P. C. J. L. Murray, "Global and regional mortality from 235 causes of death for 20 age groups in 1990 and 2010: A systematic analysis for the global burden of disease study 2010," *Lancet*, vol. 380, no. 9859, pp. 2095–2128, 2012.

[2] J. Askanazi, P. A. Silverberg, R. J. Foster, A. I. Hyman, J. Milic-Emili, and J. M. Kinney, "Effects of respiratory apparatus on breathing pattern," *J. Appl. Physiol.*, vol. 48, no. 4, pp. 577–580, 1980.

[3] B. R. Celli *et al.*, "Standards for the diagnosis and treatment of patients with COPD: A summary of the ATS/ERS position paper," *Eur. Respiratory J.*, vol. 23, no. 6, pp. 932–946, 2004.

[4] M. Folke, L. Cernerud, and M. Ekström, and B. Hök, "Critical review of non-invasive respiratory monitoring in medical care," *Med. Biol. Eng. Comput.*, vol. 41, no. 4, pp. 377–383, Jul. 2003.

[5] A. Grenvik, S. Ballou, E. McGinley, J. E. Millen, W. L. Cooley, and P. Safar, "Impedance pneumography: Comparison between chest impedance changes and respiratory volumes in 11 healthy volunteers," *Chest*, vol. 62, no. 4, pp. 439–443, 1972.

[6] K. P. Cohen, W. M. Ladd, D. M. Beams, W. S. Sheers, R. G. Radwin, W. J. Tompkins, and J. G. Webster, "Comparison of impedance and inductance ventilation sensors on adults during breathing, motion, and simulated airway obstruction," *IEEE Trans. Biomed. Eng.*, vol. 44, no. 7, pp. 555–566, Jul. 1997.

[7] J. M. Ernst, D. A. Litvack, D. L. Lozano, J. T. Cacioppo, and G. G. Berntson, "Impedance pneumography: Noise as signal in impedance cardiography," *Psychophysiology*, vol. 36, no. 3, pp. 333–338, 2010.

[8] V.-P. Seppä, J. Viik, A. Naveed, "Signal waveform agreement between spirometer and impedance pneumography of six chest band electrode configurations," in *Proc. World Congr. Med. Phys. Biomed. Eng.*, Munich, Germany, O. Dössel and W. C. Schlegel, Eds. Berlin, Germany: Springer, 2009, pp. 689–692.

[9] V.-P. Seppä, J. Viik, and J. Hyttinen, "Assessment of pulmonary flow using impedance pneumography," *IEEE Trans. Biomed. Eng.*, vol. 57, no. 9, pp. 2277–2285, Sep. 2010.

[10] V.-P. Seppä, J. Hyttinen, M. Uitto, W. Chrapek, and J. Viik, "Novel electrode configuration for highly linear impedance pneumography," *Biomedizinische Technik/Biomed. Eng.*, vol. 58, no. 1, pp. 35–38, Jan. 2013.

[11] G. Liu, G. Zhou, W. Chen, and Q. Jiang, "A principal component analysis based data fusion method for estimation of respiratory volume," *IEEE Sensors J.*, vol. 15, no. 8, pp. 4355–4364, Aug. 2015.

[12] J. H. Houtveen, P. F. C. Groot, and E. J. C. de Geus, "Validation of the thoracic impedance derived respiratory signal using multilevel analysis," *Int. J. Psychophysiol.*, vol. 59, no. 2, pp. 97–106, 2006.

[13] T. Koivumäki, M. Vauhkonen, J. T. Kuikka, and M. A. Hakulinen, "Bioimpedance-based measurement method for simultaneous acquisition of respiratory and cardiac gating signals," *Physiol. Meas.*, vol. 33, no. 8, p. 1323, 2012.

[14] H. D. Cannière, C. J. P. Smeets, P. M. Vandervoort, S. Lee, G. Squillace, M. Vandecasteele, and L. Grieten, "A wearable bioimpedance device for respiratory monitoring," in *Proc. Biomedica Life Sci. Summit*, Jun. 2015.

[15] L. P. Malmberg and V.-P. Seppä, A. Kotaniemi-Syrjänen, K. Malmström, M. Kajosaari, A. S. Pelkonen, J. Viik, and M. J. Mäkelä, "Measurement of tidal breathing flows in infants using impedance pneumography," *Eur. Respiratory J.*, vol. 49, no. 2, 2016, Art. no. 1600926.

[16] P. R. Eastwood, D. R. Hillman, and K. E. Finucane, "Ventilatory responses to inspiratory threshold loading and role of muscle fatigue in task failure," *J. Appl. Physiol.*, vol. 76, no. 1, pp. 185–195, 1994.

[17] F. Laghi, A. Topeli, and M. J. Tobin, "Does resistive loading decrease diaphragmatic contractility before task failure?" *J. Appl. Physiol.*, vol. 85, no. 3, pp. 1103–1112, 1998.

[18] Y. Kikuchi, S. Okabe, G. Tamura, W. Hida, M. Homma, K. Shirato, and T. Takishima, "Chemosensitivity and perception of dyspnea in patients with a history of near-fatal asthma," *New England J. Med.*, vol. 330, no. 19, pp. 1329–1334, 1994.

[19] P. R. Eastwood, D. R. Hillman, A. R. Morton, and K. E. Finucane, "The effects of learning on the ventilatory responses to inspiratory threshold loading," *Amer. J. Respiratory Crit. Care Med.*, vol. 158, no. 4, pp. 1190–1196, 1998.

[20] R. C. Chen, C. L. Que, and S. Yan, "Introduction to a new inspiratory threshold loading device," *Eur. Respiratory J.*, vol. 12, no. 1, pp. 208–211, 1998.

[21] C. C. Reilly, C. J. Jolley, K. Ward, V. MacBean, J. Moxham, and G. F. Rafferty, "Neural respiratory drive measured during inspiratory threshold loading and acute hypercapnia in healthy individuals," *Exp. Physiol.*, vol. 98, no. 7, pp. 1190–1198, 2013.

[22] M. Lozano-García, L. Sarlabous, J. Moxham, G. F. Rafferty, A. Torres, R. Jané, and C. J. Jolley, "Surface mechanomyography and electromyography provide non-invasive indices of inspiratory muscle force and activation in healthy subjects," *Sci. Rep.*, vol. 8, no. 1, p. 16921, Dec. 2018.

[23] F. Yang and R. P. Patterson, "The contribution of the lungs to thoracic impedance measurements: A simulation study based on a high resolution finite difference model," *Physiol. Meas.*, vol. 28, no. 7, p. S153, Jun. 2007.

[24] L. Beckmann, D. van Riesen, and S. Leonhardt, "Optimal electrode placement and frequency range selection for the detection of lung water using bioimpedance spectroscopy," in *Proc. 29th Annu. Int. Conf. IEEE Eng. Med. Biol. Soc.*, Aug. 2007, pp. 2685–2688.

[25] F. Yang and R. P. Patterson, "A simulation study on the effect of thoracic conductivity inhomogeneities on sensitivity distributions," *Ann. Biomed. Eng.*, vol. 36, no. 5, pp. 762–768, May 2008.

[26] T. Vuorela, V.-P. Seppä, J. Vanhala, and J. Hyttinen, "Design and implementation of a portable long-term physiological signal recorder," *IEEE Trans. Inf. Technol. Biomed.*, vol. 14, no. 3, pp. 718–725, May 2010.

[27] N. V. Helleputte, M. Konijnenburg, H. Kim, J. Pettine, D.-W. Jee, A. Breeschoten, A. Morgado, T. Torfs, H. de Groot, C. Van Hoof, and R. F. Yazicioglu, "18.3 A multi-parameter signal-acquisition SoC for connected personal health applications," in *Proc. IEEE Int. Solid-State Circuits Conf. (ISSCC) Dig. Tech. Papers*, Feb. 2014, pp. 314–315.

[28] American Thoracic Society/European Respiratory Society, "ATS/ERS Statement on respiratory muscle testing," *Amer. J. Respiratory Crit. Care Med.*, vol. 166, no. 4, p. 518, 2002.

[29] M.-C. Yu, J.-L. Liou, S.-W. Kuo, M.-S. Lee, and Y.-P. Hung, "Noncontact respiratory measurement of volume change using depth camera," in *Proc. Annu. Int. Conf. IEEE Eng. Med. Biol. Soc.*, Aug./Sep. 2012, pp. 2371–2374.

[30] S. Dangdang, Y. Yuting, L. Chenbin, T. Francis, Y. Hui, and T. Nongjian, "Noncontact monitoring breathing pattern, exhalation flow rate and pulse transit time," *IEEE Trans. Biomed. Eng.*, vol. 61, no. 11, pp. 2760–2767, Nov. 2014.

[31] H. Zhao, H. Hong, D. Miao, Y. Li, H. Zhang, Y. Zhang, C. Li, and X. Zhu, "A noncontact breathing disorder recognition system using 2.4-GHz digital-IF Doppler radar," *IEEE J. Biomed. Health Inform.*, vol. 23, no. 1, pp. 208–217, Jan. 2019.

DOLORES BLANCO-ALMAZÁN received the M.Sc. degree in telecommunications engineering from the Universitat Politècnica de Catalunya, Barcelona, Spain, in 2013, where she is currently pursuing the Ph.D. degree in biomedical engineering. She is also currently pursuing the joint Ph.D. degree with the Institute for Bioengineering of Catalonia (IBEC), Barcelona, and the Biomedical Research Networking Centre in Bioengineering, Biomaterials and Nanomedicine. Since 2016, she has been involved in an innovation project with the IBEC and the Holst Centre/IMEC, Eindhoven, The Netherlands. Her research interests include signal processing and interpretation, multi-sensor analysis, and data fusion in respiratory diseases.

WILLEMIJN GROENENDAAL received the master's and Ph.D. degrees from the Eindhoven University of Technology, Eindhoven, The Netherlands, in 2006 and 2011, respectively. She has been a Postdoctoral Associate with the Weill Cornell Medical College, New York, NY, USA. She is currently a Senior Researcher with the Inter-university Micro-Electronics Center (IMEC), Eindhoven, The Netherlands. Her expertise is in the interplay of physiological measurements and computational techniques.

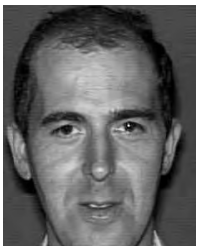

FRANCKY CATTHOOR (F'05) received the Engineering and Ph.D. degrees in electrical engineering from Katholieke Universiteit Leuven, Belgium, in 1982 and 1987, respectively.

From 1987 to 2000, he was the Head of several research domains in the areas of high-level and system synthesis techniques and architectural methodologies. Since 2000, he has been strongly involved in other activities with the Inter-University Micro-Electronics Center (IMEC), Heverlee, Belgium, including related applications and deep submicron technology aspects, biomedical imaging and sensor nodes, and smart photo-voltaic modules. Currently, he is a Fellow of the IMEC. He is a part-time Full Professor with the Department of Electrical Engineering, KU Leuven. In 1986, he has received the Young Scientist Award from the Marconi International Fellowship Council. He has been an Associate Editor of several IEEE and ACM journals such as *Transactions on VLSI Signal Processing*, *Transactions on Multimedia*, and ACM TODAES. He was the Program Chair of several conferences including ISSS 1997 and SIPS 2001. He has been elected as an IEEE Fellow, in 2005.

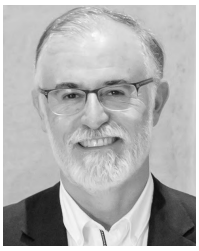

RAIMON JANÉ (M'91–SM'14) received the Ph.D. degree from the Universitat Politècnica de Catalunya (UPC), Barcelona, Spain, in 1989, where he is currently the Director of research with the Department of Automatic Control (ESAII), UPC. He is the Scientific Group Leader of the Biomedical Signal Processing and Interpretation Group, Institute for Bioengineering of Catalonia (IBEC), and the Barcelona Institute of Science and Technology (BIST), Barcelona. Since 2008, he has been the Principal Investigator of the Biomedical Signals and Systems (SISBIO) Group and a member of Steering Committee of the Biomedical Research Networking Center in Bioengineering, Biomaterials and Nanomedicine (CIBER-BBN). He is currently a Professor of the master's degree programme and the Coordinator of the Ph.D. programme in biomedical engineering. His research interests include multimodal and multiscale biomedical signal processing in cardiorespiratory diseases and sleep disorders. In 2005, he has received the Barcelona City Prize in technology research from the Barcelona City Council. He is currently a member of the IEEE EMBS Technical Committee on Cardiopulmonary Systems. He is an Associate Editor of cardiovascular and respiratory systems engineering theme of the IEEE EMBC. He has been the President of the Spanish Society of Biomedical Engineering, since 2012.